

## Realization and Measurement of a Wearable Radio Frequency Identification Tag Antenna

<sup>1,2</sup> Shudao ZHOU, <sup>1</sup> Haotian CHANG

<sup>1</sup> College of Meteorology and Oceanography, PLA Univ. of Sci. & Tech., Nanjing, 211101, China

<sup>2</sup> Collaborative Innovation Center on Forecast and Evaluation of Meteorological Disasters, Nanjing University of Information Science and Technology, Nanjing, Jiangsu, 210044, China

<sup>1</sup> Tel.: +86 025-80830101, fax: +86 025-80830101

<sup>1</sup> E-mail: zhousd70131@sina.com

*Received: 20 May 2014 /Accepted: 27 June 2014 /Published: 30 June 2014*

**Abstract:** The realization and measurements of a wearable Radio Frequency Identification tag antenna which achieves good simulation results in the Ultimate High Frequency band under the standard of the United States in design procedures is presented. The wearable tag antenna is constructed using a flexible substrate, on whose surface the antenna patch is adhered. A bowtie shape is chosen as the geometry of the antenna patch because of its large bandwidth that brings to the tag and its simple structure. The substrate of the tag antenna is realized using a foam material while the patch on the substrate surface is cut out from copper foil tape. Then, the impedance of the realized tag antenna is extracted from S parameters which are measured with a vector network analyzer with a coaxial fixture. Finally, the radiation pattern of the tag is characterized by normalized reading distances of different directions of the antenna integrated with a microchip, thus indicating the validity of the realized tag antenna. *Copyright © 2014 IFSA Publishing, S. L.*

**Keywords:** Wearable, Radio frequency identification, Tag antenna, Reading distance, Directivity.

### 1. Introduction

Radio Frequency Identification (RFID) is widely used in logistics, manufactures, biomonitors. Applications of RFID are realized in Sensor Networks and healthcare, which are attractive because of the battery-less features. RFID systems mainly consist of two parts, readers and tags [1]. Passive tags receive interrogation signals from readers, from which the Radio Frequency (RF) power required to the tags is derived, and send signals which are modulated by the tags themselves. Since wearable RFID tags are fabricated in clothes and the tag antennas do not transmit but backscatter the interrogation signals from the readers, they need to scavenge energy effectively and remain in small dimensions while being adhered to lossy human

body, which requires good impedance match between antennas and microchips.

In this paper, a wearable RFID antenna is realized. Measurements are carried out so as to understand the performances of the tag. Results of reading distances and radiation pattern are presented, as well as the analysis of the results of the antenna between simulation and measurements.

### 2. Design and Simulation Results

#### 2.1. Geometry of the Antenna Patch

The impedance of antenna which achieves a large bandwidth needs to remain steady within the working

frequency band. The wave energy reflected from the boundary of antenna and free space will account for a small proportion of the total wave energy if the length of antenna is longer than the wavelength, which means most of the wave energy is radiated out to the free space. Because the impedance of bowtie antenna sustains a constant value in a large frequency band, which prevents wave energy being reflected from the truncation of the antenna, bowtie geometry is adopted as the pattern of the antenna patch.

## 2.2. Modeling of the Antenna via Simulation Software

As discussed above, due to the requirements of achieving a wide bandwidth, the bowtie geometry is adopted. The antenna is modeled via High Frequency Structure Simulator (HFSS) of Ansoft. The geometrical center of the patch pattern locates in the center of the upper surface of the substrate, and the bowtie lies along the Y-axis. As depicted in Fig. 1, the antenna modeled via HFSS is shown below.

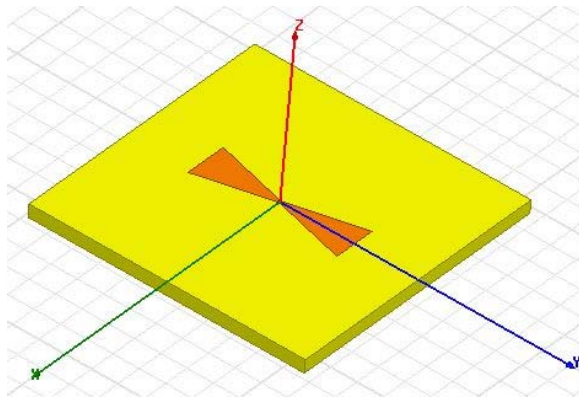


Fig. 1. Modeling of the antenna via HFSS.

Each arm of the bowtie has a length signed as arm length along Y-axis and the distance between the two arms is signed as port gap width. Additionally, the lengths of the upper and lower edges of the two arms are signed as inner width and outer width, respectively.

Because the RFID tag mainly works in far fields, we insert Infinite Sphere in Radiation Setup. The solution frequency is 915 MHz, the standard of RFID of the U.S.

## 2.3. Optimization Results of the Antenna

After sweeping the parametric of the patch pattern, we find that the S11 parameters are sensitive to arm length. Hence, arm length is signed as the optimizing parameter. We set up the optimization goal as VSWR less than 1, under which circumstance the reflecting wave energy aims to remain the lowest level.

The optimized antenna shows good simulation results. As shown in Fig. 2, although the central frequency moves slightly to 919 MHz (an offset of 4 MHz), the frequency band that S11 is less than -10dB attains almost 140 MHz, which achieves a satisfactory bandwidth.

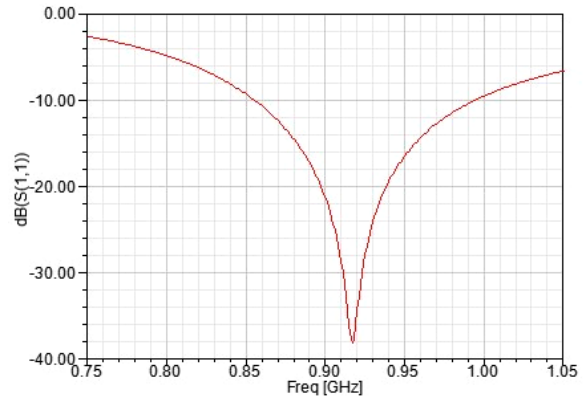


Fig. 2. S11 parameter of the optimized antenna.

The VSWR of the antenna hits the bottom at 1.0571 at 915 MHz, which means the reflecting energy takes up only 2.8 % of the total wave energy scavenged by the antenna, as shown in Fig. 3. In addition, the radiation pattern on XOY plane is a spindle-like shape and it is a circle on XOZ plane, which is similar to the radiation pattern of dipole antenna, as shown in Fig. 4. The input impedance of the wave port is  $49.7+j1.3 \Omega$ .

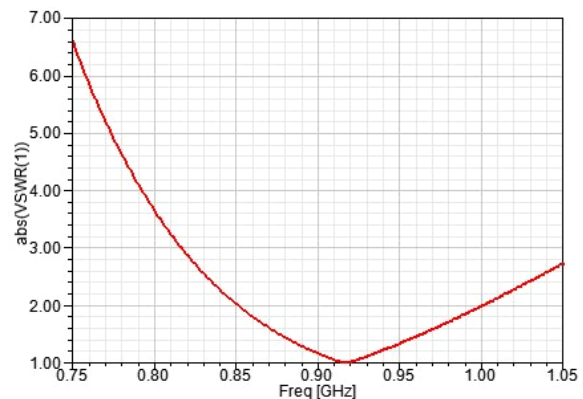


Fig. 3. VSWR of the optimized antenna.

## 3. Realization of the Antenna

The substrate is made from a foam material through a foaming mould which is 210 mm in both length and width. We have three foaming moulds with different thickness, which are 1mm, 5 mm and 10 mm thick, respectively. In order to achieve good flexibility, the mould we adopt is the thinnest, which is only 1 mm in thickness.

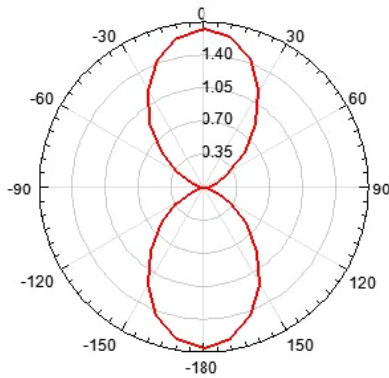


Fig. 4. Directivity of the optimized antenna on XOZ plane.

The foam material is composed by two liquid organic materials. After being mixed, the foam material is poured into the foaming mould. The foaming procedure takes nearly one hour, during which period of time the foam material turns solid. The relative permittivity of the foam material is 1.2 and its loss tangent value is 0.0027.

As the patch pattern is assigned as a perfect conductor boundary, the patch pattern is realized with thin copper foil tape with a bulk conductivity of 58000000 S/m, which can be approximately regarded as a perfect E plate.

In order to acquire the patch with precise sizes, the bowtie geometry is depicted in CAD and printed on paper at first. The printed pattern is cut out after clinging to a copper foil tape, thus the copper patch is acquired. Then, the copper patch is adhered to the upper surface of the substrate after being separated from the paper beneath the foil tape.

Finally, the microchip is placed in the center of the substrate and is coupled with the two bowtie arms by silver conductive adhesive. The realized tag is shown in Fig. 5.



Fig. 5. Realized tag.

## 4. Measurements of the Realized Antenna

### 4.1. Impedance of the Realized Antenna

As discussed above, the power-off reading distance depends on the wave energy scavenged from the interrogation signal and then the energy the antenna acquired from the microchip. If the impedance of the antenna and the microchip achieve

a conjugation, the RF signal will be most effectively scavenged, thus increasing the power-off reading distance of the RFID tag. Therefore, measurements of the impedance of the antenna without being coupled to the microchip are carried on.

The measurement methodology is based on S parameters. The equivalent network of an asymmetrical dipole antenna is shown in Fig. 6 [3].

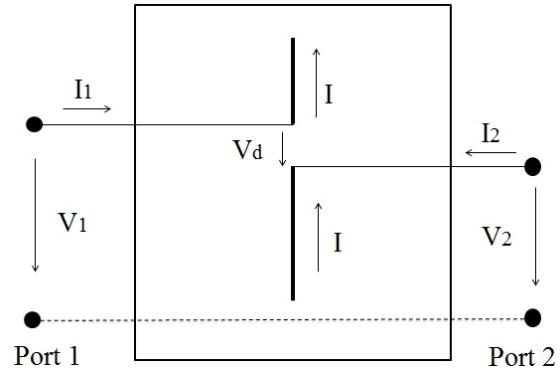


Fig. 6. Equivalent network.

The differential impedance of the antenna can be expressed as:

$$Z_d = \frac{V_d}{I} = \frac{V_1 - V_2}{I}, \quad (1)$$

where  $Z_d$  is the differential impedance,  $V_d$  is the differential voltage of the input, and  $I$  is the current through the antenna.

The voltages of the ports can be expressed by Z parameters as:

$$V_1 = Z_{11}I_1 + Z_{12}I_2, \quad (2)$$

$$V_2 = Z_{21}I_1 + Z_{22}I_2, \quad (3)$$

Transforming Z parameters to S parameters, the differential impedance can be expressed as:

$$Z_d = \frac{2Z_0(1 - S_{11}S_{22} + S_{12}S_{21} - S_{12} - S_{21})}{(1 - S_{11})(1 - S_{22}) - S_{21}S_{12}}, \quad (4)$$

where  $Z_0$  is the characterized impedance.

For symmetrical antennas,  $S_{11}$  equals to  $S_{22}$  and  $S_{12}$  equals to  $S_{21}$ . The equation above can be simplified to Equation (5).

$$Z_d = \frac{2Z_0(1 - S_{11}^2 + S_{21}^2 - 2S_{12})}{(1 - S_{11})^2 - S_{21}^2}, \quad (5)$$

Based on the measurement methodology invented by Xianming Qing, etc., the balanced antenna is coupled to the two ports of a two-port VNA through a fixture, because the impedance of balanced antennas cannot be measured directly by instruments

which are terminated with unbalanced ports [4]. The fixture consists of two coaxial cables whose outer conductors are soldered together. There are two SMA connectors on one end of the fixture, which are connected to the ports of the VNA through test cables. The inner conductors on the other end of the fixture are slightly longer than the outer conductors so as to connect the wave port of the antenna from the lower surface of the substrate. The prototype of the fixture is fabricated with two semi-ridge coaxial cables, both of which are 100 mm in length and have the same diameter of outer conductor of 2.2 mm. the prototype of the fixture is shown in Fig. 7.

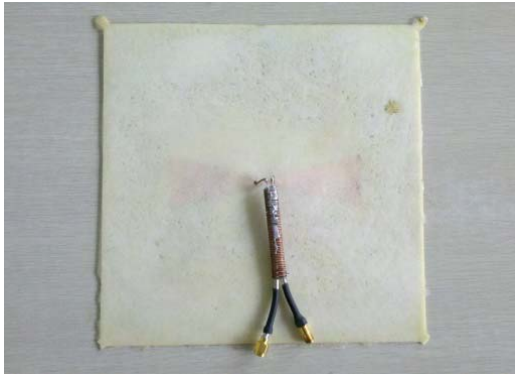


Fig. 7. Demonstration of the fixture.

Although the VNA provides accurate measurement results under standard calibration, the standard calibration only exists at the ends of the test cables. Furthermore, the fixture brings about frequency-dependent phase delay and loss, thus inflicting the accuracy of measurement. In order to de-embed the influence of the fixture, the calibration plane is moved from the ends of the fixture, the calibration plane is moved from the ends of the test cables to the ends of the inner conductors of the fixture. Therefore, when the antenna is connected to the inner conductors of the fixture, S parameters of the antenna are measured correctly by the VNA. The results of S parameters are shown in Fig. 8.

Finally, the impedance of the antenna is figured out from the measured S parameters, using Equation (5). The impedance of the antenna is  $83.72-j16.66 \Omega$ .

#### 4.2. Measurements of the Radiation Pattern

The measurements of the radiation pattern are performed with an Alien ALR-9900 reader and a TI RI-UHF-STRAP-08 microchip.

The reader and the tag are placed in the same ground level. The tag is adhered to a wooden board which is equipped with a pointer vertically placed to the substrate plane and a protractor, thus indicating the direction of the normal vector of the upper substrate plane.



Fig. 8(a). S11 parameter of the tag.



Fig. 8(b). S12 parameter of the tag.



Fig. 8(c). S21 parameter of the tag.



Fig. 8(d). S22 parameter of the tag.

Firstly, the tag is placed as the Y-axis parallel to the ground. The power-off reading distances of different directions are measured, as presented in Table 1. Then, the radiation pattern is characterized by the normalized reading distances, as shown in Fig. 9. Then the tag is placed as the Y-axis vertical to the ground, under which circumstance the power-off reading distances of different directions are shown in Table 2.

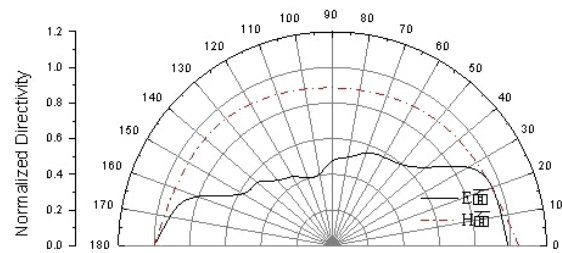


Fig. 9. Directivity of the realized tag.

Table 1. Reading distances of different directions with Y-axis parallel to the ground

0°	10°	20°	30°	40°	50°	60°	70°	80°	90°
191 cm	187 cm	187 cm	180 cm	180 cm	130 cm	114 cm	112 cm	110 cm	96 cm
100°	110°	120°	130°	140°	150°	160°	170°	180°	
77 cm	77 cm	89 cm	90 cm	113 cm	102 cm	170 cm	180 cm	194 cm	

Table 2. Reading distances with Y-axis vertical to the ground

0°	45°	90°	135°	180°
326 cm	320 cm	300 cm	328 cm	312 cm

Normalized reading distances which are measured with the Y-axis of the antenna vertical to the ground indicate the directivity in XOZ plane (H plane), while the reading distances which are measured with the Y-axis parallel to the ground indicate the directivity in YOZ plane (E plane). From Fig. 6, we can see that the directivity in XOZ plane has a good consensus with the simulation result which appears to be a circle, while the directivity in YOZ plane does not show a spindle-like shape as the simulation result does. But the directivity on YOZ plane shows that the normalized directivity decreases from 0degree to 90degree and increase from 90 degree to 180 degree, whose monotonicity is similar with that of the simulation result. The realized tag achieves a good performance of reading distance, which attains at 3.28 m at most in H plane.

## 5. Conclusion

The influences that geometry sizes bring to antenna performances can be easily simulated and analyzed through HFSS, by which the optimization of antennas can also be easily carried on. Optimization mainly on the aspect of arm length helps to acquire the most satisfactory design properties of the bowtie antenna. The results of the performances of optimized antenna show a good

radiation pattern and a wide bandwidth of 140 MHz that the S11 is below -10 dB. The designed antenna has a thin thickness and a simple structure, which is easy to realize in practice. By measuring the power-off reading distances of different directions, the radiation pattern is characterized, which shows a good directivity on H plane. Even though the impedance of the antenna and the microchip does not match a conjugation, the largest power-off reading distance of the tag reaches 3.28 m, thus proving the validity of the realized tag.

## References

- [1]. S. Cecilia Ochiuzzi, T. Stefano Cippitelli, Gaetano Marrocco, Design and Experimentation of Wearable RFID Sensor Tag, *IEEE Transactions on Antennas and Propagation*, Vol. 58, Issue 8, 2010, pp. 2490-2498.
- [2]. S. Sabina Manzari, T. Cecilia. Occhiuzzi, and Gaetano Marrocco, Feasibility of Body-Centric Systems Using Passive Textile RFID Tags, *IEEE Antennas and Propagation Magazine*, Vol. 54, Issue 4, 2012, pp. 49-62.
- [3]. S. Xianming. Qing, T. Chean Khan Goh, and Zhi Ning Chen, Impedance Characterization of Asymmetrical Balanced Antennas and Application in RFID Tag Design, *IEEE Transaction, Microwave Theory and Technique*, Vol. 57, Issue 5, 2009, pp. 1268-1274.
- [4]. T. Xianming Qing, T. Chean Khan Goh, Zhi Ning Chen, Measurement of UHF RFID Tag Antenna Impedance, in *Proceedings of the IEEE International Workshop on Antenna Technology (iWAT'09)*, Santa Monica, CA, 2-4 March 2009, Paris, France, 16-19 March 2003, pp. 1-4.